Effect of Arginine-48 Replacement on the Reaction between Cytochrome *c* Peroxidase and Hydrogen Peroxide†

Lidia B. Vitello,‡ James E. Erman,*,‡ Mark A. Miller,§ Jimin Wang,§,⊥ and Joseph Kraut§

Departments of Chemistry, Northern Illinois University, DeKalb, Illinois 60115, and University of California at San Diego, La Jolla, California 92093

Received March 18, 1993; Revised Manuscript Received June 25, 1993®

ABSTRACT: The crystallographic structures of two cytochrome *c* peroxidase (CcP) mutants, CcP(R48L) and CcP(R48K), have been determined. In addition, the electronic absorption spectrum and the hydrogen peroxide reactivity of these two mutants have been determined between pH 4 and 8. Both the crystallographic structure and the electronic absorption spectrum of CcP(R48L) are consistent with exclusive pentacoordination of the heme iron between pH 4 and 6.5. At higher pH, CcP(R48L) forms an alkaline bis-imidazole form of CcP with the distal histidine coordinated to the heme iron. The apparent pK_A for this transition is 7.5 in CcP(R48L). The observed pseudo-first-order rate constant for the reaction between CcP(R48L) and hydrogen peroxide saturates at high peroxide concentrations. The data are consistent with a rate-limiting oxygen–oxygen bond scission at high peroxide concentrations. The observed rate of the bond scission step ranges between 1000 and 1950 s^{-1}, an estimated 2 orders of magnitude slower than for wild-type enzyme. The data suggest that the protonated form of His-52 increases the bond scission step by a factor of 2. The properties of the CcP(R48K) mutant are significantly different from those of CcP(R48L). The crystal structure of CcP(R48K) shows Lys-48 occupying the putative peroxide binding site. The electronic absorption spectrum indicates that CcP(R48K) is predominantly pentacoordinate at neutral pH but with detectable amounts of hexacoordinate forms. Two ionizable groups affect the electronic absorption spectrum of CcP(R48K). An apparent ionization near pH 4 produces an enzyme with increased hexacoordination, while an apparent pK_A of 6.9 generates the alkaline bis-imidazole form. The peroxide reaction saturates at high peroxide concentrations for CcP(R48K) and is attributed to a conformational-gating mechanism. The maximum rate for the reaction between CcP(R48K) and hydrogen peroxide is probably limited by the movement of either Lys-48 or His-52. This rate is 200 and 290 s^{-1} in nitrate-containing buffers and phosphate buffers, respectively. Evidence is provided that Arg-48 in wild-type enzyme is responsible for nitrate binding in the heme pocket and for stabilizing CcP Compound I.

In the preceding paper (Erman *et al.*, 1993), we investigated the role of the distal histidine, His-52, on the rate of cytochrome *c* peroxidase Compound I formation and found that replacement of His-52 with a leucine residue decreases the bimolecular rate of Compound I formation by 5 orders of magnitude and enhances the endogenous decay of Compound I by 2–3 orders of magnitude. A second distal residue, Arg-48, has been invoked as a catalytic residue for Compound I formation (Poulos & Kraut, 1980). It has been proposed that the positively charged Arg-48 stabilizes the transition state for Compound I formation through electrostatic interaction with the developing negative charge on the distal oxygen of the bound peroxide during heterolytic oxygen–oxygen bond cleavage. Replacing Arg-48 with a leucine residue removes the positive charge and the possibility of hydrogen bonding at this position. If these two properties are important, we would expect a substantial decrease in the rate of O–O bond cleavage. Replacing Arg-48 with a lysine residue preserves the positive charge, although the exact position of the charge may be altered as well as the hydrogen-bonding pattern. We would anticipate a smaller effect of the lysine mutation on the hydrogen peroxide reaction rate, and this is what is found. At low hydrogen peroxide concentrations, the Lys-48 mutant retains more than 50% of the wild-type activity while the Leu-48 mutant is only 2% as active as CcP(YST).[1] These relatively small changes in the rate of Compound I formation compared to those for the Leu-52 mutant (Erman *et al.*, 1992, 1993) are at first surprising. However, upon further consideration of the mechanism of hydrogen peroxide activation, these results are quite reasonable.

The reaction between hydrogen peroxide and CcP is best visualized as occurring via a two-step mechanism, eqs 1 and 2. In the first step, hydrogen peroxide binds to the heme iron,

$$\mathrm{CcP} + \mathrm{H_2O_2} \underset{k_d}{\overset{k_a}{\rightleftarrows}} \mathrm{HCcP{\cdot}O_2H} \qquad (1)$$

$$\mathrm{HCcP{\cdot}O_2H} \xrightarrow{k_c} \mathrm{CcP{\cdot}I} + \mathrm{H_2O} \qquad (2)$$

and in the second step, the O–O bond is cleaved, producing Compound I and water. The O–O bond cleavage step is very fast for wild-type peroxidases, probably on the order of 10^5

† This work was supported in part by Research Grants PHS 1R15 DK43944 to L.B.V. and J.E.E. and NSF MCB 9119292 to J.K.

* Author to whom correspondence should be addressed.

‡ Northern Illinois University.

§ University of California at San Diego.

⊥ Current Address: Department of Molecular Biophysics and Biochemistry, KBT-234, P.O. Box 6666, Yale University, 219 Prospect St., New Haven, CT 06511.

® Abstract published in *Advance ACS Abstracts,* September 1, 1993.

[1] Abbreviations: CcP, cytochrome *c* peroxidase; CcP(YST), wild-type cytochrome *c* peroxidase from yeast; CcP(MI), recombinant cytochrome *c* peroxidase expressed in *Escherichia coli*; CcP(R48L), the Arg-48→Leu mutant of CcP(MI); CcP(R48K), the Arg-48→Lys mutant of CcP(MI); CT1 and CT2, charge-transfer bands in the electronic absorption spectrum of CcP; MPD, 2-methyl-2,4-pentanediol.

0006-2960/93/0432-9807$04.00/0

s^{-1} at room temperature (Balny *et al.*, 1987b). Under typical stopped-flow conditions, keeping the observed pseudo-first-order rate constant less than about 300 s^{-1}, the association of hydrogen peroxide is the rate-limiting step in the mechanism. The concentration of the CcP–hydrogen peroxide complex is very small under these conditions. Using a steady-state approximation for the CcP–hydrogen peroxide complex, the observed pseudo-first-order rate constant, k_A, is given by eq 3.[2] Equation 3 predicts a hyperbolic dependence of k_A on the

$$k_A = k_c k_a[H_2O_2]/(k_a[H_2O_2] + k_c + k_d) \quad (3)$$

peroxide concentration with the maximum value of k_A (k_A^{max}) equal to k_c at infinite peroxide. At low peroxide concentrations, the apparent bimolecular rate constant is given by eq 4. For

$$k_1^{app} = k_a k_c/(k_c + k_d) \quad (4)$$

CcP(YST), k_d is likely to be much smaller than k_c, and k_1^{app} is essentially equal to k_a, the true association rate constant. Since k_c appears as the ratio $k_c/(k_d + k_c)$ in eq 4, k_c will have little influence on k_1^{app}. In CcP mutants, k_c would have to become comparable in value to k_d in order to have a significant effect on k_1^{app}.

The most important function of His-52 is to accept a proton from the incoming hydrogen peroxide to facilitate the binding of the peroxide anion to the Fe(III) heme, and mutations at this site have the greatest influence on k_a, which is directly proportional to the experimentally observed apparent bimolecular rate constant, k_1^{app}. Replacement of His-52 with a leucine residue decreases k_1^{app} by 5 orders of magnitude (Erman *et al.*, 1992, 1993).

The most important function of Arg-48 is thought to be promotion of O–O heterolysis by stabilizing the transition state in the second step of the mechanism. Mutations at position 48 will have their greatest influence on k_c, but their effect will have little influence on k_1^{app} unless k_c becomes comparable to the dissociation rate of the peroxide, k_d, or if the mutation directly influences k_a. However, if the mutation at position 48 decreases the rate of O–O bond heterolysis by 2–3 orders of magnitude, then k_c in the mutant enzymes may be detectable by stopped-flow techniques at room temperature. The reactions of both CcP(R48K) and CcP(R48L) with hydrogen peroxide saturate at high peroxide concentrations with maximum rates of 290 and 1950 s^{-1}, respectively. The maximum rate for the CcP(R48L) mutant most likely represents the rate of O–O bond scission, k_c, but the maximum rate for CcP(R48K) is probably associated with conformational changes within the protein. In either case, the observed maximum first-order rate constants provide lower limits for the rate of O–O bond scission for both mutants. The CcP(R48L) mutant also provides evidence that the protonated form of His-52 may participate in O–O heterolysis through stabilization of the transition state and donation of a proton to the departing hydroxide ion.

MATERIALS AND METHODS

Twice-crystallized CcP(R48L) and CcP(R48K) were prepared as previously described (Fishel *et al.*, 1987; Smulevich *et al.*, 1988). Concentrations of the enzymes were determined spectroscopically in 0.1 M phosphate buffer, pH 6, using a millimolar absorptivity of 97 at 405 nm and 105 at 411 nm for CcP(R48L) and CcP(R48K), respectively (Smulevich *et al.*, 1988).

All other reagents and experimental methods were as described previously (Erman *et al.*, 1993), including the two buffer systems used in this study. The first buffer system was 10 mM in either acetate or phosphate with added KNO_3 to adjust ionic strength to 0.1 M. The second buffer system was 0.1 M in total phosphate concentration.

Both CcP(R48K) and CcP(R48L) mutant enzymes were crystallized from sitting drops of 30% 2-methyl-2,4-pentanediol (MPD) buffered with 50 mM potassium phosphate at pH 6.0, as described for the parent CcP(MI) (Wang *et al.*, 1990). The crystals are isomorphous to the parent CcP(MI) in space group $P2_12_12_1$, and unit cell dimensions were within experimental error of the parent: 104.88 Å × 74.24 Å × 45.53 Å.

X-ray diffraction data for both CcP(R48K) and CcP(R48L) mutants were collected at the UCSD area detector resource center (Xuong *et al.*, 1985). A complete 2.0-Å data set for CcP(R48K) was processed from 171 558 observations for two single crystals, yielding 22 951 unique reflections with R_{sym} = 4.7.[3] For CcP(R48L), data were only completed to 2.5 Å due to rapid deterioration of the crystal in the X-ray beam. Deterioration of these crystals was at least 10 times faster than that of the parent CcP(MI) crystals. The data set was processed from 126 954 observations from one single crystal, yielding 15 996 unique reflections with R_{sym} = 7.1. Average intensity changes from CcP(MI) to CcP(R48K) and to CcP(R48L) were 12.1% (to 2.0 Å) and 15.0% (2.5 Å), respectively.

Both mutant structures were well refined, with *R*-factors of 16.4% (2.0 Å) for CcP(R48K) and 15.9% (2.5 Å) for CcP(R48L), with reasonable geometry restraints (0.012–0.014 Å for bond length deviations). Coordinates of both structures have been deposited in the Brookhaven Protein Data bank under the names 6CCP (mutant R48L) and 7CCP (mutant R48K). More detailed structure refinement and geometry analysis have been described by Wang (1988).

RESULTS

Crystal Structure of CcP(R48L). The difference Fourier map, F_o[CcP(R48L)] – F_o[parent], is shown superimposed on the structure of the CcP(MI) parent in Figure 1A. The most important feature in the map is a peak of negative density near position 48, which results from the decrease in side-chain mass accompanying the substitution of leucine for arginine and the loss of water-595. Structure refinement clearly showed that water-595 is absent and that the iron is displaced from the mean porphyrin plane by 0.4 Å toward the proximal side. This represents an additional 0.2-Å movement of the iron out of the porphyrin plane relative to CcP(MI) (Wang *et al.*, 1990). The side chain of His-175 follows the movement of the iron, and the geometries of the imidazole ligand are not changed as a result. The refined structure of the mutant CcP(R48L) is superimposed upon the CcP(MI) parent in Figure 1B.

Spectrum of CcP(R48L). The spectrum of CcP(R48L) is identical, within experimental error, in the two buffer systems used in this study. The spectrum of the mutant enzyme depends upon pH, and spectra obtained at pH 6 and 8 are shown in Figure 2. Spectral properties at these two pH values are given in Table I. The midpoint for the interconversion between the acid and alkaline forms of the enzyme occurs at

[2] A more rigorous derivation, eliminating the steady-state approximation, gives $k_A = 0.5(k_a[H_2O_2] + k_c + k_d) - ((k_a[H_2O_2] + k_c + k_d)^2 - 4k_a k_c[H_2O_2])^{1/2}$. The limiting values of k_A at low and high hydrogen peroxide concentrations are the same as those given by eq 3.

[3] $R_{sym} = \sum_{hkl}(\sum_i |I_i - \bar{I}|/\sum_i I_i$ where I_i is the observed intensity of the *i*th reflection, and $\bar{I}$ is the scaled mean intensity.

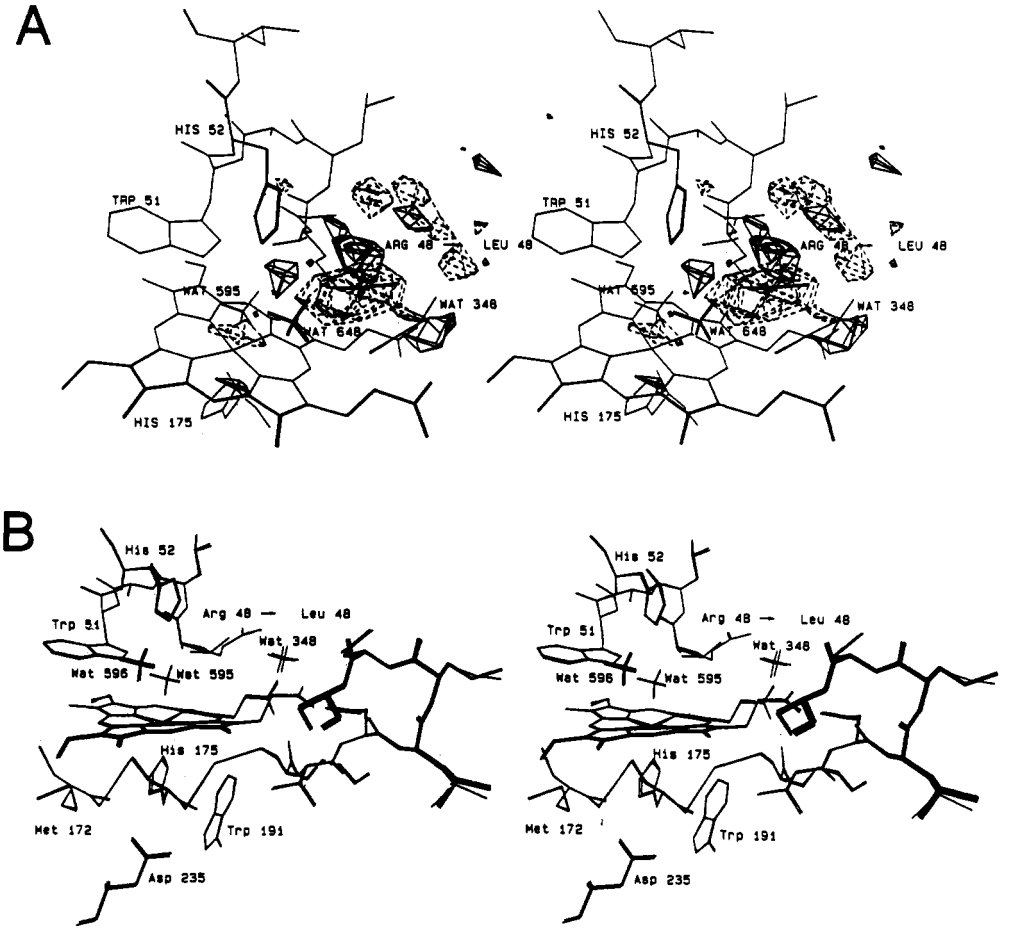

FIGURE 1: Heme cleft region of CcP(R48L). (A) Difference Fourier map, F_o[CcP(R48L)] – F_o[CcP(MI)] contoured at 3.5σ, superimposed on the refined CcP(MI) model. Solid lines represent positive density features, and dashed lines are negative. Tetrahedra represent solvent water molecules. (B) Refined active-site structure of CcP(R48L) superimposed upon the CcP(MI) model. The depth-cued lines represent the CcP(MI) parent. Tetrahedra represent solvent water molecules. Water-595 is shown for the CcP(MI) parent model only and is not assigned for CcP(R48L).

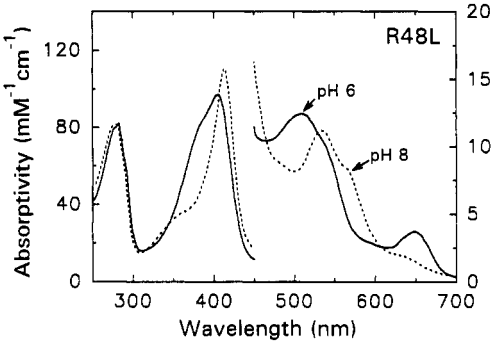

FIGURE 2: Spectrum of CcP(R48L) in 0.1 M phosphate buffers at pH 6.0 and 8.0.

about pH 7.4 in both buffer systems. The solid line in Figure 3 is calculated according to a mechanism presented below.

Reaction between CcP(R48L) and Hydrogen Peroxide. When hydrogen peroxide is added to CcP(R48L), an increase in absorbance at 424 nm, due to Compound I formation, is observed (Figure 4). The absorbance increase is followed by a relatively rapid decrease in absorbance in this mutant, and this decrease is attributed to the endogenous decay of Compound I (Erman & Yonetani, 1975a,b). At low hydrogen peroxide concentrations (≤100 μM), the pseudo-first-order constant for Compound I formation, k_A, is independent of the buffer composition and increases with increasing peroxide concentration (Figure 5A). At high hydrogen peroxide concentrations (up to 10 mM), k_A tends to saturate, reaching a limiting value as predicted by eq 3 (see Figure 5B). Values of k_1^{app} (eq 4) and k_A^{max} (equivalent to k_c in eq 3) were determined by fitting k_A to eq 3 using nonlinear least-squares regression. A third parameter, K^{app}, is defined in eq 5. K^{app}

$$K^{app} = k_A^{max}/k_1^{app} \quad (5)$$

has the units of concentration, and in this context, values of K^{app} are equivalent to the hydrogen peroxide concentrations which cause k_A to equal one-half of k_A^{max}. Values of K^{app} increase from 2.0 mM at pH 7.5 to 58 mM at pH 5.0. At pH 4.0 and 4.5, we did not observe saturation in k_A up to 10 mM hydrogen peroxide and this is attributed to the weaker apparent association of hydrogen peroxide and CcP(R48L) at these pH values. At pH 8, we were able to observe the rate of Compound I formation only at low hydrogen peroxide concentrations, apparently due to rapid oxidation of the heme at the higher peroxide concentrations.

pH Dependence of k_1^{app} and k_A^{max}. The apparent bimolecular rate constant and the maximum observed rate for the reaction between hydrogen peroxide and CcP(R48L) are both dependent upon pH (Figure 6A,B). The values of k_1^{app} for the hydrogen peroxide/CcP(R48L) reaction were independent of the buffer system, within experimental error, between pH 4.5 and 8.0. At pH 4, k_1^{app} is somewhat larger in nitrate-containing buffer (Figure 6A). This is in contrast to the behavior of CcP(YST) and CcP(MI), where the hydrogen peroxide reaction is significantly slower at low pH in nitrate-containing buffer as compared to phosphate buffer. Data for CcP(YST) in both buffer systems are included in Figure 6A for comparison with CcP(R48L). The specific ion effects in the CcP(YST)/hydrogen peroxide reaction have been asso-

Table I: Spectroscopic Parameters of CcP(R48L) and CcP(R48K)[a]

protein	pH/buffer	δ	Soret	CT2	β	α	CT1
CcP(R48L)	4.0/KNO_3	378 (78.7,sh)	404 (101)	508 (12.2)	542 (9.0,sh)		647 (3.9)
CcP(R48L)	4.0/KPhos	378 (77.3,sh)	404 (98.0)	508 (12.4)	542 (9.2,sh)		646 (3.8)
CcP(R48L)	6.0/KNO_3	378 (75.4,sh)	405 (97.5)	510 (12.6)	543 (9.5,sh)		649 (3.8)
CcP(R48L)	6.0/KPhos	378 (78.1,sh)	405 (97.0)	510 (12.5)	543 (9.5,sh)		648 (4.0)
CcP(R48L)	8.0/KNO_3	360 (40.5,sh)	414 (107)		534 (10.7)	566 (8.1,sh)	635 (1.9,sh)
CcP(R48L)	8.0/KPhos	360 (43.6,sh)	414 (110)		534 (11.2)	566 (8.4,sh)	635 (1.9)
CcP(R48K)	4.0/KNO_3	360 (36.8,sh)	410 (116)	530 (9.9)		570 (6.0,sh)	636 (2.3)
CcP(R48K)	4.0/KPhos	360 (36.5)	410 (118)	528 (9.8)		570 (6.0,sh)	630 (2.6)
CcP(R48K)	6.0/KNO_3	380 (58.1,sh)	413 (109)	525 (11.1)	541 (10.4,sh)		645 (2.3)
CcP(R48K)	6.0/KPhos	378 (61.3,sh)	411 (105)	520 (11.2)	542 (10.1,sh)		647 (2.8)
CcP(R48K)	8.0/KNO_3	358 (28.4)	414 (124)		534 (11.6)	566 (9.1,sh)	
CcP(R48K)	8.0/KPhos	358 (28.2)	413 (127)		534 (11.4)	566 (8.9,sh)	

[a] Wavelength maximum given in nanometers, followed by millimolar absorptivity in parentheses.

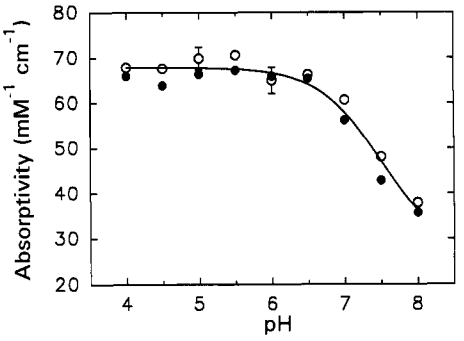

FIGURE 3: Absorptivity of CcP(R48L) at 370 nm as a function of pH. Solid circles, nitrate-containing buffers. Open circles, 0.1 M phosphate buffers. The solid line was calculated from the mechanism shown in Figure 14 and the parameters collected in Table II.

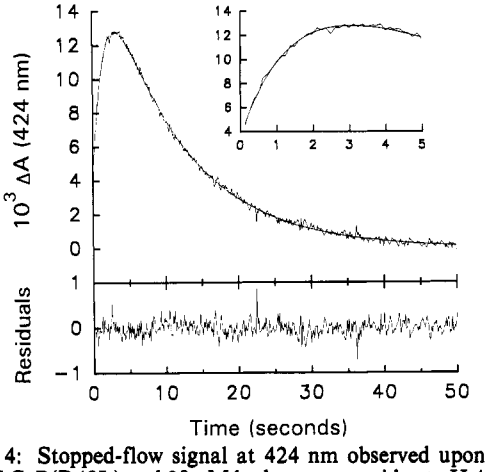

FIGURE 4: Stopped-flow signal at 424 nm observed upon mixing 0.68 μM CcP(R48L) and 38 μM hydrogen peroxide at pH 4.0 in 0.1 M phosphate buffer. The increase in absorbance is due to Compound I formation, and the decrease in absorbance is due to the endogenous decay of Compound I. The data were fit to a two-exponential equation and yielded rate constants of 0.672 and 0.0954 s^{-1} for k_A and k_{decay}, respectively. The residuals between calculated and experimental data are shown in the bottom panel.

ciated with nitrate binding in the distal heme pocket, stabilizing the protonated form of His-52 (Vitello *et al.*, 1990b; Erman *et al.*, 1993).

Values of k_A^{max} also vary with pH (Figure 6B) decreasing from a values of 2150 ± 850 s^{-1} at pH 5 to 1090 ± 110 s^{-1} at pH 7.5. The solid lines in Figure 6A,B were calculated from a mechanism presented below.

The amplitude of the reaction observed in the stopped-flow system is shown in Figure 6C. The amplitude of the reaction is independent of the hydrogen peroxide concentration (below 100 μM) between pH 5 and 8 but depends upon the hydrogen peroxide concentration in a hyperbolic manner at pH 4 and

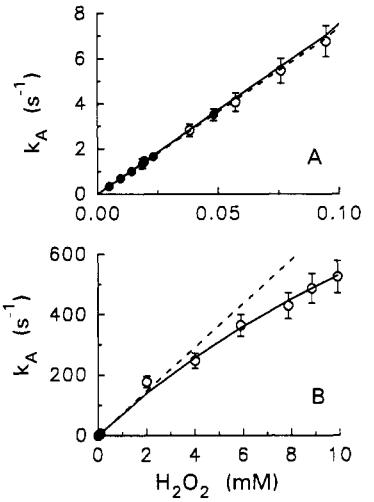

FIGURE 5: Dependence of k_A, the pseudo-first-order rate constant for CcP(R48L) Compound I formation, on the hydrogen peroxide concentration at pH 5.5. Solid circles, nitrate-containing buffer. Open circles, 0.1 M phosphate buffers. (A) 5–100 μM hydrogen peroxide. (B) 0.005–10 mM hydrogen peroxide.

4.5. The values plotted in Figure 6C are the maximum values for the absorbance changes. The hydrogen peroxide concentrations that give half-maximal amplitudes are 39 and 9.4 μM at pH 4 and 4.5, respectively. The amplitude of the hydrogen peroxide/CCP(R48L) reaction essentially mirrors the pH dependence of the absorbance in the electronic absorption spectrum (Figure 3). No reaction was observed at pH 8.4 or above.

The very rapid decay of the CcP(R48L) Compound I (Figure 4) precludes static titration of this mutant by hydrogen peroxide, and the stoichiometry of the enzyme/hydrogen peroxide reaction cannot be determined. However, the amplitude of the reaction between the mutant and hydrogen peroxide to form Compound I gives the absorptivity difference between the mutant enzyme and its oxidized intermediate. These absorptivity values average 43 ± 1 mM^{-1} cm^{-1} at 424 nm between pH 4 and 6.5 (Figure 6C). We cannot determine the fraction of mutant converted to Compound I under these conditions since we do not know the absorptivity of CcP(R48L) Compound I, but we do note that the observed amplitude is about 80% of the absorptivity difference for conversion of CcP(YST) to Compound I. We can conclude that a significant fraction of CcP(R48L) is converted to Compound I between pH 4 and 6.5.

Endogenous Decay of CcP(R48L) Compound I. The endogenous decay of CcP(R48L) Compound I is significantly more rapid than that of Compounds I of CcP(YST) or CcP(MI). The decay is complex, with at least two resolvable phases over the pH range between 4 and 8. There is a fast

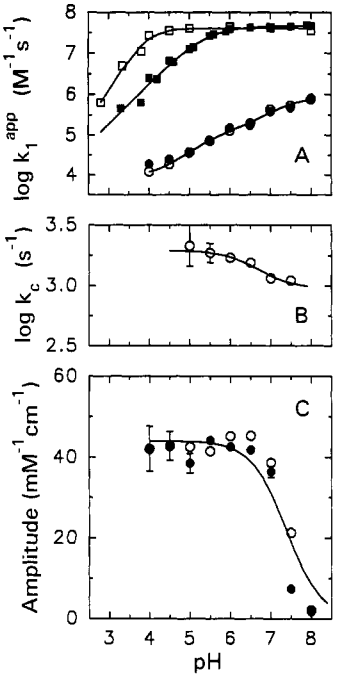

FIGURE 6: (A) pH dependence of the apparent bimolecular rate constant for CcP Compound I formation. Solid circles, CcP(R48L) in nitrate-containing buffer. Open circles, CcP(R48L) in 0.1 M phosphate buffers. Solid squares, CcP(YST) in nitrate-containing buffers [data from Loo & Erman (1975)]. Open squares, CcP(YST) in 0.1 M phosphate buffers. (B) Values of k_A^{max} for the CcP(R48L)/hydrogen peroxide reaction in 0.1 M phosphate buffer. (C) Amplitude of the stopped-flow traces for CcP(R48L) Compound I formation as a function of pH. Solid circles, 0.1 M ionic strength nitrate-containing buffer. Open circles, 0.1 M phosphate buffer. All solid lines for the CcP(R48L) data in this figure were calculated on the basis of the mechanism shown in Figure 14 and the parameters shown in Table II.

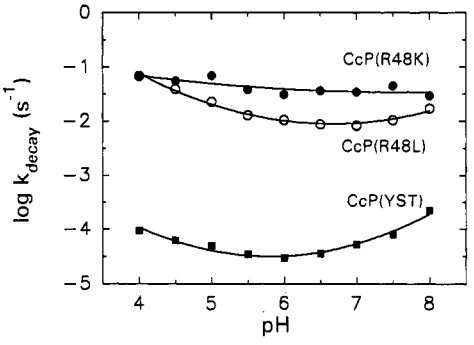

FIGURE 7: Rate of the endogenous decay of CcP Compound I as a function of pH. In general, the decay is biphasic, and the data shown are for the major decay phase. Open circles, CcP(R48L). Solid circles, CcP(R48K). Solid squares, CcP(YST). All data were collected in nitrate-containing buffer.

decay phase which accounts for 57–95% of the decay amplitude, depending upon the pH. The rate constant for this phase of the decay reaction is relatively independent of pH, varying from a low of 0.030 s^{-1} at pH 8 to a high of 0.070 s^{-1} at pH 5 (Figure 7). The slow phase of the reaction, which makes a minor contribution to the amplitude of the decay, is 4–12 times slower than the fast phase, varying from 0.0024 to 0.0094 s^{-1} at pH 8 and 5.5, respectively. Figure 7 includes data on the decay of CcP(YST) Compound I, and it can be seen that CcP(R48L) Compound I is 2–3 orders of magnitude less stable than oxidized wild-type enzyme.

Crystal Structure of CcP(R48K). The difference Fourier map, F_o(R48K) – F_o(parent), is shown superimposed on the structure of the CcP(MI) parent in Figure 8A. The dominant features of the difference density map were confined to the immediate vicinity of the mutation. The largest positive peak in the map appears near residues 48 and 52 and the iron coordination site. The largest negative peak appears in the location of the guanidinium moiety of Arg-48, and the second largest negative peak is located near His-52 (Figure 8A). It is clear that the side chains of residues 48 and 52 are displaced toward each other (from negative density features toward positive) in the CcP(R48K) structure.

The changes in the enzyme structure accompanying the Arg-48→Lys mutation were examined by unbiased difference Fourier studies (Wang, 1988) and subsequent refinement. Based on $F_o - F_c$ difference maps, where the densities for water-595 and Arg-48 were omitted from the calculations, substitution of Lys-48 for Arg can be clearly seen (Figure 8B). The side chain of Lys-48 is positioned between His-52 and the heme iron. The ϵ-amino group of Lys-48 is 2.7 Å away from the iron and occupies the position of water-595 in the parent structure. The portion of the guanidinium moiety of Arg-48 that interacts with water-348 in the parent structure is replaced by a new water molecule, water-784.

The structural changes accompanying the substitution of Lys for Arg-48 also perturb the orientation of the imidazole side chain of His-52. In the CcP(R48K) enzyme, a movement of His-52 by 0.3 Å toward residues 81 and 82 is seen, accompanied by small adjustments along the backbone (Figure 8C). In addition, the $F_o - F_c$ map of CcP(R48K) (Figure 8B) suggests that a rotation of the His-52 side chain by 180° about the C_β–C_γ bond may occur in at least some fraction of the enzyme population. This rotation would allow N_ϵ of His-52 to interact with the Ser-81 backbone carbonyl oxygen and remove N_δ from the position that interacts readily with water-595 or approaching peroxide ligands. Note, however, that this rotation would also place N_δ within 2.4 Å of the carbonyl oxygen of Ser-81, a distance that is shorter than any known hydrogen bond. Unfortunately, the data do not permit us to evaluate the extent to which this rotation has occurred.

Spectrum of CcP(R48K). The spectrum of CcP(R48K) varies to a greater extent as a function of pH and buffer composition than does that of CcP(R48L) or CcP(YST). The spectrum of CcP(R48K) changes continually over the pH range 4–8. Spectra of CcP(R48K) in 0.1 M phosphate buffer at pH 4, 6, and 8 are shown in Figure 9. Spectroscopic parameters in both buffer systems are collected in Table I. A plot of the absorptivity at 370 nm as a function of pH is shown in Figure 10. It is evident that at least three forms of the enzyme exist between pH 4 and 8. The pH dependence of the spectrum can be quantitatively fit to a titration curve involving two enzyme ionizations which produce spectrally distinct acidic, neutral, and alkaline forms of the enzyme. The solid lines in Figure 10 were calculated from a mechanism to be presented later.

The spectrum of the CcP(R48K) is sensitive to the buffer composition and differs to the greatest extent at pH 6 in the two buffer systems used in this study. At pH 4 and 8, the spectrum of the mutant enzyme is essentially the same in the two buffer systems (Table I).

Reaction between CcP(R48K) and Hydrogen Peroxide. The reaction between CcP(R48K) and hydrogen peroxide is complex. Two distinct kinetic phases are observed for Compound I formation between pH 4.5 and 8.0, and both of these phases saturate at relatively low peroxide concentrations (Figure 11). We can characterize the hyperbolic hydrogen peroxide dependence by two kinetic parameters. The limiting slope at low hydrogen peroxide concentrations gives an apparent bimolecular rate constant for the reaction between CcP(R48K) and hydrogen peroxide, k_1^{app} from k_A and k_2^{app}

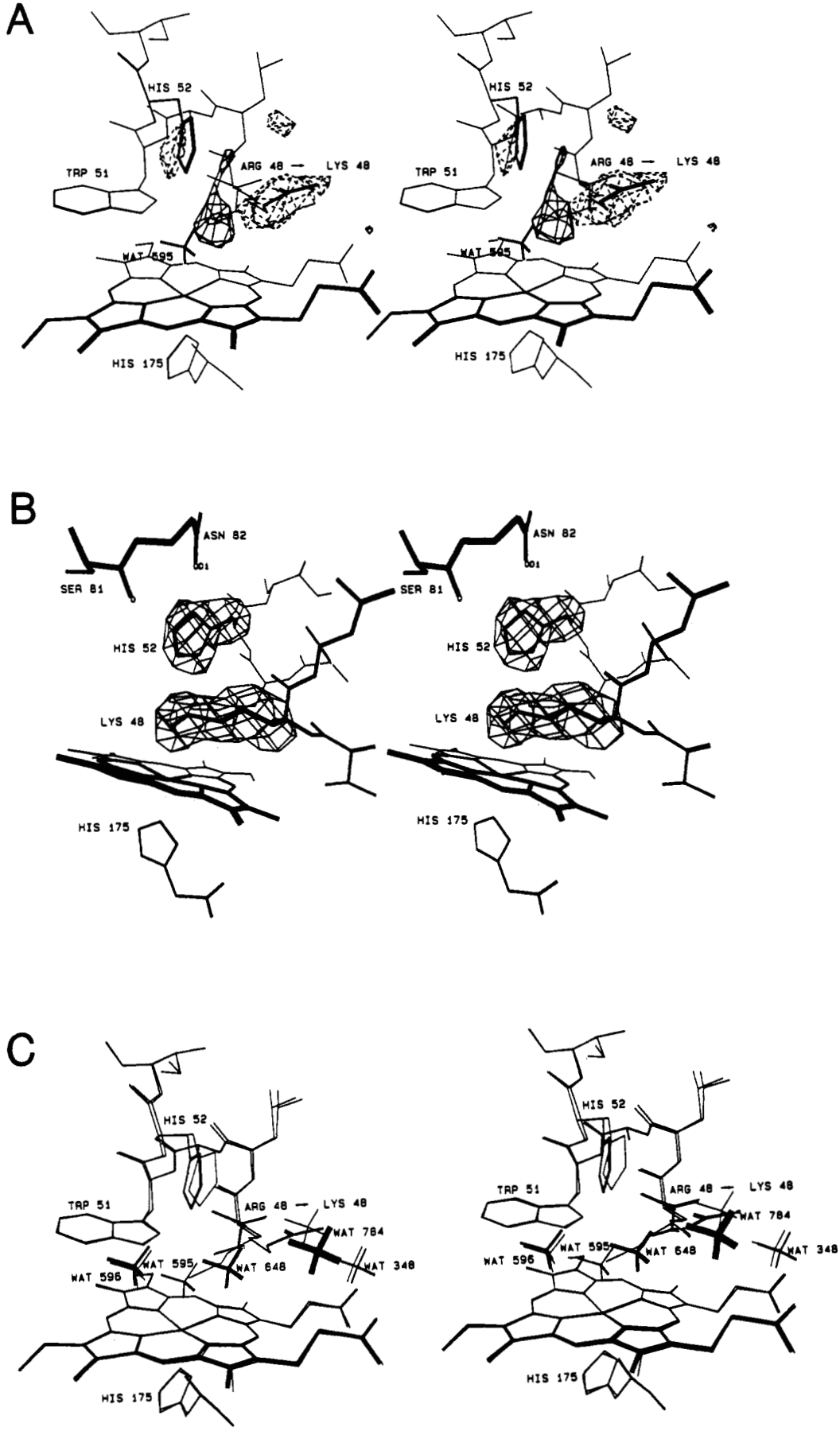

FIGURE 8: Heme cleft region of CcP(R48K). (A) Difference Fourier map, F_o[CcP(R48K)] – F_o[CcP(MI)] contoured at 3.5σ, superimposed on the refined CcP(MI) model. Solid lines represent positive density features, and dashed line are negative. Tetrahedra represent solvent water molecules. (B) Difference Fourier map, $F_o - F_c$ calculated for CcP(R48K) after omitting the coordinates for Arg-48 and His-52. The map is superimposed upon the final refined structure of CcP(R48K). (C) Refined active-site structure of CcP(R48K) superimposed upon the CcP(MI) model. The depth-cued lines represent the CcP(MI) parent. Tetrahedra represent solvent water molecules.

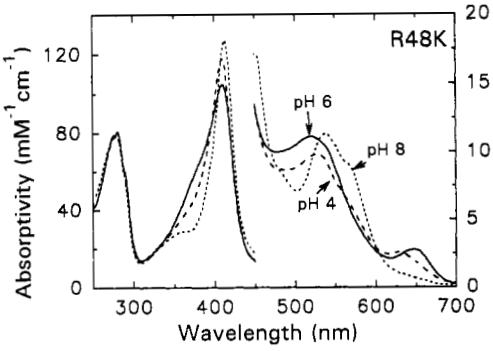

FIGURE 9: Spectrum of CcP(R48K) in 0.1 M phosphate buffers at pH 4, 6, and 8.

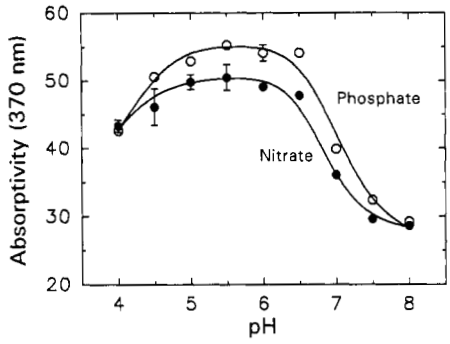

FIGURE 10: pH dependence of the absorptivity at 370 nm for CcP(R48K). Solid circles, nitrate-containing buffer. Open circles, 0.1 M phosphate. The solid lines were calculated according to the mechanism shown in Figure 15 and pK_A values collected in Table III.

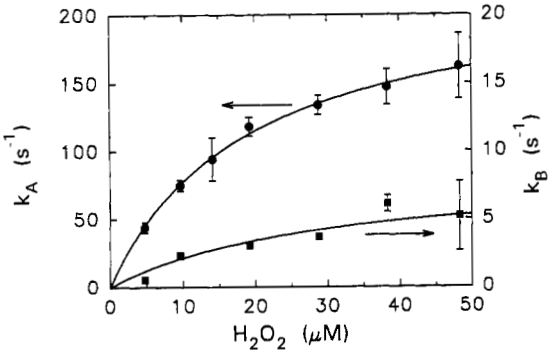

FIGURE 11: Dependence of k_A, the pseudo-first-order rate constant for the fast phase of CcP(R48K) Compound I formation, and k_B, the pseudo-first-order rate constant for the slow phase of CcP(R48K) Compound I formation, on the hydrogen peroxide concentration. Solid circles, k_A, left-hand ordinate. Solid squares, k_B, right-hand ordinate. Data were collected in 0.1 M ionic strength nitrate-containing buffer, pH 5.5.

from k_B, while the limiting rate at high hydrogen peroxide concentrations gives a maximum first-order rate for Compound I formation, k_A^{max} and k_B^{max} from k_A and k_B, respectively.

The fastest of the two phases, with rate constant k_A, is associated with the largest change in absorbance over most of the pH range (Figure 12). The amplitude of the fast phase has a bell-shaped dependence on pH with a maximum near pH 5. This bell-shaped dependence provides evidence for at least two enzyme ionizations influencing the hydrogen peroxide reaction. The slow reaction phase, with rate constant k_B, is generally a small fraction of the total reaction amplitude. The amplitude of the slow reaction is essentially independent of pH between pH 4.5 and 8 (Figure 12).

All four kinetic parameters depend upon the pH, and the pH dependence in nitrate-containing buffers is shown in Figure 12. The kinetic parameters for the CcP(R48K) hydrogen peroxide reaction are dependent upon specific ion effects. The

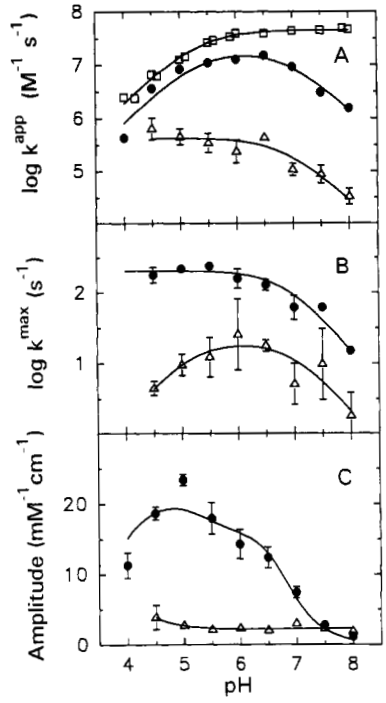

FIGURE 12: pH dependence of the kinetic parameters for CcP(R48K) Compound I formation in nitrate-containing buffers. (A)Solid circles, k_1^{app}, the apparent bimolecular rate constant for the fast phase of CcP(R48K) Compound I formation. Open triangles, k_2^{app}, the apparent bimolecular rate constant for the slow phase of CcP(R48K) Compound I formation. Open squares, the apparent bimolecular rate constant for CcP(YST) Compound I formation [data from Loo & Erman (1975)]. (B) Solid circles, k_A^{max}, the maximum value of k_A at infinite hydrogen peroxide concentration. Open triangles, k_B^{max}, the maximum value of k_B at infinite hydrogen peroxide concentration. (C) Amplitude of the fast and slow phases for CcP(R48K) Compound I formation. Solid circles, fast phase associated with rate constant k_A. Open triangles, slow phase associated with rate constant k_B. The solid lines for the major phase, k_A, of the CcP(R48K)/hydrogen peroxide reaction were calculated according to the mechanism shown in Figure 15 and the parameters collected in Table III.

kinetic parameters observed in phosphate buffers are shown in Figure 13. While the overall behavior of the reaction is similar in both phosphate and nitrate-containing buffers, the apparent pK_as and pH-independent rate constants differ somewhat in the two buffer systems.

Endogenous Decay of CcP(R48K) Compound I. The decay of CcP(R48K) is biphasic over the pH range 4–8. The fast decay phase accounts for 63–89% of the reaction amplitude between pH 4 and 7.5, with rate constants varying between 0.0083 and 0.068 s^{-1} (Figure 7). The slow decay phase, with a rate of 0.0043 s^{-1}, accounts for 68% of the decay amplitude at pH 8. CcP(R48K) Compound I is somewhat more stable than that of CcP(R48L) but is 2–3 orders of magnitude less stable than CcP(YST) Compound I (Figure 7).

DISCUSSION

Heme Ligation of CcP(R48L). The structure of the CcP(R48L) mutant shows that replacement of Arg-48 by Leu decreases the occupancy of water-595 dramatically and causes the iron atom to move by 0.2 Å toward the proximal side of the heme plane. The structural changes observed for CcP(R48L) are consistent with resonance Raman data that indicate that this mutant is exclusively pentacoordinate at acid pH (Smulevich *et al.*, 1988). If it is assumed that the movement of water-595 into the coordination sphere of the iron produces the hexacoordinate high-spin form of the parent CcP(MI) at acidic pH, then the Arg-48→Leu mutation would shift the equilibrium toward pentacoordination simply by

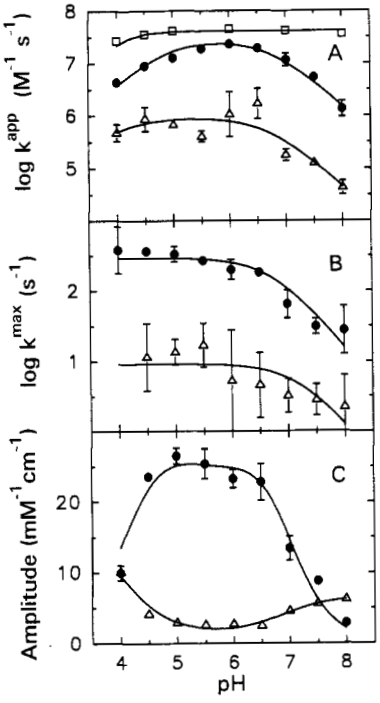

FIGURE 13: pH dependence of the kinetic parameters for CcP(R48K) Compound I formation in 0.1 M phosphate buffers. (A) Solid circles, k_1^{app}, the apparent bimolecular rate constant for the fast phase of CcP(R48K) Compound I formation. Open triangles, k_2^{app}, the apparent bimolecular rate constant for the slow phase of CcP(R48K) Compound I formation. Open squares, the apparent bimolecular rate constant for CcP(YST) Compound I formation. (B) Solid circles, k_A^{max}, the maximum value of k_A at infinite hydrogen peroxide concentration. Open triangles, k_B^{max}, the maximum value of k_B at infinite hydrogen peroxide concentration. (C) Amplitude of the fast and slow phases for CcP(R48K) Compound I formation. Solid circles, fast phase associated with rate constant k_A. Open triangles, slow phase associated with rate constant, k_B. The solid lines for the major phase, k_A, of the CcP(R48K)/hydrogen peroxide reaction were calculated according to the mechanism shown in Figure 15 and the parameters collected in Table III.

decreasing the occupancy of water-595. Additional factors which could contribute to the absence of a hexacoordinate form of CcP(R48L) at acidic pH include the loss of the positively charged guanidinium side chain, which stabilizes iron–ligand interactions (Erman & Vitello, unpublished data), and the displacement of the iron toward the proximal base by an additional 0.2 Å from the heme plane, which may impose a steric hindrance to ligand binding.

The electronic absorption spectrum of CcP(R48L) is consistent with exclusive pentacoordination of the heme iron between pH 4 and 6.5 (Figures 2 and 3). The Soret/380-nm ratio for CcP(R48L) is 1.24, significantly smaller than those for CcP(YST) and CcP(MI), which are 1.51 and 1.53, respectively, at pH 6.0 (Vitello *et al.*, 1990a,b), and about the same as those for CcP(H52L) (Erman *et al.*, 1993). Higher values of this absorbance ratio correlate with increasing amounts of hexacoordination (Yonetani & Anni, 1987).

As the pH of the solution is increased above pH 6.5, the spectrum of CcP(R48L) changes to that of a hexacoordinate low-spin form (Figures 2 and 3). The spectrum of the alkaline form of CcP(R48L) is similar to those of the alkaline form of CcP(YST) and all CcP mutants observed to date, with the exception of CcP(H52L) (Smulevich *et al.*, 1991). This alkaline enzyme form has the distal histidine coordinated to the heme iron (Smulevich *et al.*, 1991). The pH dependence of the spectrum of CcP(R48L) (Figure 3) is consistent with a single enzyme ionization controlling the conversion between the acid and alkaline forms of this mutant. The apparent pK_A for the acid/alkaline isomerization is 7.5 ± 0.1.

Heme Ligation of CcP(R48K). The pH dependence of heme ligation of CcP(R48K) is somewhat more complicated than CcP(R48L). At least three spectroscopic forms of CcP(R48K) exist between pH 4 and 8 (Figures 9 and 10). At neutral pH, the spectroscopic properties suggest that CcP(R48K) is predominantly pentacoordinate, but a small amount of hexacoordinate species is present (Figure 9; Smulevich *et al.*, 1988). The Soret/380-nm absorbance ratio is 1.64, somewhat higher than the values for CcP(YST) and CcP(MI) and considerably higher than the value of 1.24 for CcP(R48L). Resonance Raman studies detect small amounts of hexacoordinate forms at neutral pH for CcP(R48K) as well as for CcP(YST) and CcP(MI) (Smulevich *et al.*, 1988, 1989). As the pH is decreased from 6 to 4, the neutral form of CcP(R48K) is partially converted to an acidic form (Figure 10). Both the neutral and acid forms of the enzyme appear to be mixtures of penta- and hexacoordinate high-spin species with a larger hexacoordinate component at low pH. The most likely ligand for the hexacoordinate high-spin species is a water molecule. The alkaline bis-imidazole form of CcP(R48K) is produced as the pH is increased from 6 to 8.

The crystal structure of CcP(R48K) is consistent with pentacoordination of the heme iron. The side chain of Lys-48 extends toward the heme iron, and the ε-amino group of Lys-48 occupies essentially the same position as water-595 in pentacoordinate CcP(MI). The ε-amino group of Lys-48 is 2.7 Å from the heme iron, too far for coordination.

The close proximity of the ε-amino group of Lys-48 to the positively charged iron suggests that this residue is unprotonated. Moreover, it appears that Lys-48 is deprotonated in the solution form of CcP(R48K) under the conditions of crystallization. The absorption spectrum of CcP(R48K) dissolved in mother liquor (see Materials and Methods) shows that the enzyme is predominantly in the alkaline low-spin form. Apparently, crystallization stabilizes a pentacoordinate form of the enzyme over the hexacoordinate form that predominates in solution under the conditions of crystallization.

These observations suggest that the crystal structure of CcP(R48K) is representative of the pentacoordinate population that reacts with peroxide below pH 7.0, but two aspects of this structure distinguish it from other mutants previously examined. These may be relevant to the unusual saturation of the peroxide reaction at low peroxide concentrations. First, the conformation of Lys-48 in the crystal structure may block the access of peroxide to the iron. We believe that the location of the Lys-48 side chain could depend upon its protonation state. In the crystal structure, Lys-48 is unprotonated and lies about 2.7 Å from the heme iron. In the protonated state, the Lys-48 side chain would be more favorably positioned near the heme propionates, as is Arg-48 in wild-type CcP. A hydrogen-bonding interaction between ε-amino group of Lys-48 and water-348 can be achieved by simple rotations of the side chain about the C_β–C_γ bonds. Such a movement would restore the accessibility of the iron to approaching peroxide. The two conformations could exert a gating effect of the reaction of CcP(R48K) with ligands. Second, the possibility of two conformations for His-52 is a distinctive characteristic of the CcP(R48K) structure. The data shown in Figure 8B suggest that the imidazole side chain may rotate by 180° relative to the orientation of His-52 in the CcP(MI) parent. In view of the critical role for His-52 in the reaction with peroxide [see accompanying paper, Erman *et al.* (1993)], a rotation of this side chain about C_γ may decrease the rate of reaction with peroxide dramatically. This would provide a second potential conformational gating mechanism.

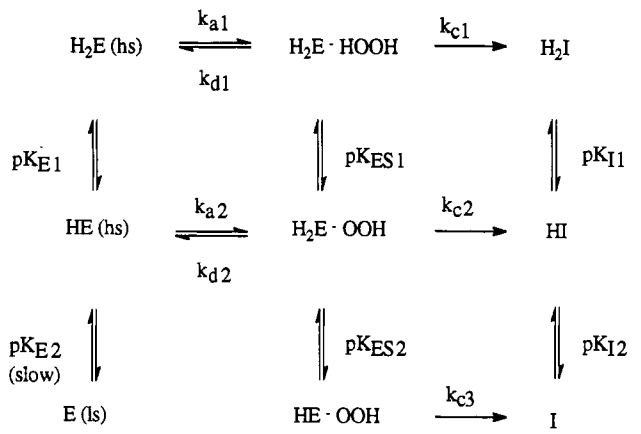

FIGURE 14: Mechanism used to explain the pH dependence of the spectroscopic and kinetic parameters of CcP(R48L). Two ionizable groups in the enzyme are required, and the groups associated with pK_{E1} and pK_{E2} are His-52 and His-181, respectively. Deprotonation of His-181 promotes formation of the alkaline low-spin hexacoordinate bisimidazole form of CcP(R48L) represented by E(ls) in the mechanism. E(ls) interconverts slowly with HE(hs) and is not converted to Compound I on the time scale of the hydrogen peroxide reaction. In the enzyme–peroxide complex, pK_{ES1} and pK_{ES2} represent deprotonation of the Fe(III)-bound hydrogen peroxide and His-52, respectively. Best-fit values of the parameters defined in the figure are collected in Table II. The parameters are independent of the nature of the buffer.

Table II: Kinetic Parameters for the Reaction between CcP(R48L) and Hydrogen Peroxide[a]

rate constant	value	apparent pK_A	value
k_{a1} (M^{-1} s^{-1})	$(3.52 \pm 0.77) \times 10^4$	pK_{E1}	5.78 ± 0.16
k_{a2} (M^{-1} s^{-1})	$(8.20 \pm 0.71) \times 10^5$	pK_{E2}	7.48 ± 0.09
$k_{c1} = k_{c2}$ (s^{-1})	1950 ± 60	pK_{ES1}	6.87 ± 0.13
k_{c3} (s^{-1})	1010 ± 50	pK_{ES2}	6.00 ± 0.11
k_{d1} (s^{-1})	5810 ± 2960		
k_{d2} (s^{-1})	11000 ± 5600		

[a] Parameters defined in Figure 14 of the text. The parameters are independent of the buffer system used in this study.

Mechanism of CcP(R48L) Compound I Formation. At any given pH, the kinetic data for CcP(R48L) are consistent with the two-step mechanism shown in eqs 1 and 2, where hydrogen peroxide binds to the heme iron in the first step and oxygen–oxygen bond cleavage occurs in the second step. Assuming that the enzyme–hydrogen peroxide complex is in a steady state, the observed pseudo-first-order rate constant is given by eq 3. The pH dependence of the kinetic and spectroscopic properties indicates that various protonated states of CcP(R48L) must be involved. The simplest mechanism to explain the pH dependence of both the kinetic and spectroscopic data is shown in Figure 14. A minimum set of kinetic parameters and apparent acid dissociation constants are defined in Figure 14 and Table II. Best-fit parameters were obtained by simultaneously fitting the pH dependence of k_1^{app} and k_A^{max}, the amplitude of the kinetic reaction, and the spectroscopic changes using nonlinear least-squares regression. The best-fit parameters are collected in Table II, and these parameters were used to calculate the theoretical lines in Figures 3 and 6.

Three ionized forms of CcP(R48L) are required to fit the data. These are represented by H_2E(hs), HE(hs), and E(ls) in Figure 14. Both H_2E(hs) and HE(hs) are pentacoordinate forms of the mutant enzyme and are related by the ionization associated with pK_{E1}. The best-fit value of pK_{E1} is 5.78 ± 0.16 (Table II), and we attribute this ionization to His-52. The ionization of His-52 has no effect on the spectroscopic properties of CcP(R48L) but does promote the association of hydrogen peroxide. Conversion of the acidic high-spin form to the alkaline low-spin bis-imidazole form of CcP(R48L) is due to the ionization of the group associated with pK_{E2}. We tentatively identify this group with His-181, since His-181 has been implicated in formation of the alkaline hexacoordinate low-spin form of ferrousCcP (Miller *et al.*, 1990). Conversion of pentacoordinate CcP to the bis-imidazole form involves significant conformational changes in the protein, and the apparent ionization constant pK_{E2} includes contributions from conformational equilibria (Dhaliwal & Erman, 1985). Because the ionization of His-181 affects the amplitude of the reaction but not the pH dependence of k_1^{app}, interconversion of HE(hs) and E(ls) (Figure 14) must be slow on the time scale of the hydrogen peroxide reaction, and the bis-imidazole form does not react with hydrogen peroxide.

Hydrogen peroxide reacts preferentially with HE(hs) in the mechanism, and this is the species with the basic form of His-52. Unprotonated His-52 acts as a proton acceptor as hydrogen peroxide binds, and the species represented by $H_2E{\cdot}OOH$ in Figure 14 has a protonated His-52 and the peroxide anion bound to the heme iron. We need to consider three protonation states of the enzyme–peroxide complex. The protonated form of His-52 can dissociate to give HE·OOH, associated with pK_{ES2} in Figure 14. In addition, the iron-bound peroxide anion can bind a proton, pK_{ES1}, to generate species $H_2E{\cdot}HOOH$ in Figure 14. The rate of O–O bond heterolysis is given by k_A^{max}, and the pH dependence of k_A^{max} is determined by k_{c1}, k_{c2}, k_{c3}, pK_{ES1}, and pK_{ES2} in Figure 14. Maximal O–O bond scission occurs when His-52 is protonated with a rate of 1950 s^{-1}. When His-52 is ionized at more alkaline pH, the rate of O–O cleavage decreases by a factor of 2, to about 1000 s^{-1}. These data provide evidence that His-52 can participate in the bond scission step.

The data suggest that hydrogen peroxide can dissociate from the enzyme only when His-52 is protonated, presumably to donate a proton to the departing peroxide anion. The rate of dissociation at acidic pH varies between 5800 and 11 000 s^{-1} and becomes undetectable at higher pH, when both the bound peroxide and His-52 are unprotonated. The dissociation rate of 11 000 s^{-1} is about 6 times faster than the cleavage of the O–O bond to form Compound I, indicating that at low pH, the mechanism of Compound I formation approaches one of rapid-equilibrium binding of hydrogen peroxide to CcP(R48L), followed by a rate-limiting O–O bond cleavage.

Mechanism of CcP(R48K) Compound I Formation. The reaction between CcP(R48K) and hydrogen peroxide to form Compound I is biphasic. We attribute this to the presence of two conformational states in the mutant enzyme that interconvert very slowly (or not at all) compared to the reaction with hydrogen peroxide. The conformational state which reacts with hydrogen peroxide at the slower rate represents about 5–10% of the total enzyme, independent of pH. It may be related to the slowly reacting phase sometimes seen in "aged" samples of CcP(YST) (Balny *et al.*, 1987a; Yonetani & Anni, 1987), although alternative explanations are possible. In any event, since it represents such a small fraction of the total enzyme, we will not discuss it in detail but instead will concentrate on the major phase of the hydrogen peroxide reaction.

There are two major differences in the reaction of CcP(R48K) with hydrogen peroxide in comparison to that of CcP(YST). The first is that the observed pseudo-first-order rate constant for the mutant enzyme/hydrogen peroxide reaction saturates at relatively low peroxide concentrations (Figure 11). The second is the bell-shaped pH dependence of k_1^{app} for CcP(R48K), which requires that two ionizable enzyme

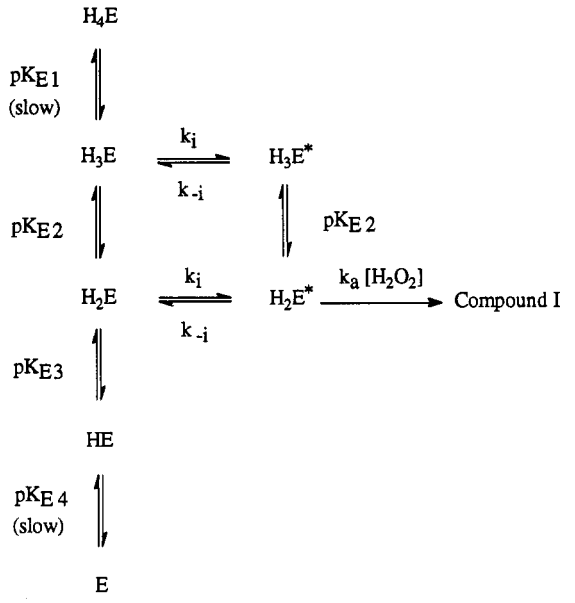

FIGURE 15: Mechanism used to explain the pH dependence of the kinetic and spectroscopic properties of CcP(R48K). Species represented by E through H_4E represent a "closed" conformation which cannot react with hydrogen peroxide directly. These closed forms of CcP(R48K) represent essentially all of the resting-state enzyme, and k_{-i} is much greater than k_i. The isomerization rate k_i limits the rate of the hydrogen peroxide reaction at high peroxide concentrations. Species H_2E^* and H_3E^* represent "open" forms of the enzyme which react with hydrogen peroxide when His-52 is deprotonated. pK_{E2}, pK_{E3}, and pK_{E4} represent the ionizations of His-52, Lys-48, and His-181, respectively. pK_{E1} represents an unknown group which converts CcP(R48K) into an unreactive acidic form of the enzyme. The apparent ionizations associated with pK_{E1} and pK_{E2} are slow on the time scale of the hydrogen peroxide reaction, and species E and H_4E are not converted to Compound I. The best-fit values for the parameters defined in the figure are collected in Table III and depend upon the nature of the buffer.

groups influence the rate of reaction with hydrogen peroxide (Figure 12A), unlike CcP(YST) and CcP(MI), which are maximally reactive in this pH range when a single group is deprotonated. CcP(R48K) requires one group in its basic form and the other in its acidic form to get maximal reactivity. By analogy to CCP(YST) and CcP(R48L), His-52 is the group that functions as a general base. We argue below that Lys-48 is the group that must be protonated for maximal activity.

Although the two-step mechanism presented in eqs 1 and 2 predicts that the observed pseudo-first-order rate constant k_A should saturate at high peroxide concentrations (eq 3) with a limiting value of k_c, the rate of O–O heterolysis, we do not believe that this is the correct interpretation for the CcP(R48K) data. There are several lines of evidence which suggest that k_A^{max} is not a measure of the rate of O–O heterolysis; the strongest is that k_A^{max} for CcP(R48L) is greater than k_A^{max} for CcP(R48K). If k_A^{max} were a measure of k_c for both mutants, we would expect k_A^{max} for the Leu-48 mutant to be substantially smaller than for the Lys-48 mutant, since it is difficult to envision how the leucine residue could promote heterolysis better than a positively charged lysine residue. Additionally, the crystallographic structure of CcP(R48K) shows Lys-48 blocking the hydrogen peroxide binding site. This suggests that significant conformational changes in protein structure must occur during the reaction with hydrogen peroxide and conformational gating may be limiting the reaction at high peroxide concentrations. Such a conformational-gating mechanism is shown in Figure 15.

The mechanism shown in Figure 15 describes several conformational and protonated forms of the enzyme. The minimal mechanism requires three ionized forms in rapid equilibrium to account for the bell-shaped pH dependence of k_1^{app} (Figures 12A and 13A). Two additional ionized states which interconvert slowly on the peroxide reaction time scale are required to explain the pH dependence of the amplitude of the reaction (Figures 12C and 13C). The five protonated species, E through H_4E, related through apparent acid dissociation constants, pK_{E1} through pK_{E4}, in Figure 15 represent various protonated forms of a "closed" conformational state. Species H_3E^* and H_2E^* represent the "open" conformation. We equate pK_{E2} with the ionization of His-52 in both the closed and open states. Hydrogen peroxide only reacts with enzyme species having an open conformational state and, when His-52 is unprotonated, species H_2E^* in Figure 15. The data suggest that the fraction of closed-conformation enzyme is greater than 90% in the resting-state enzyme.

In our mechanism, the protonation state of Lys-48 is critical in the formation of the closed and open conformations. When Lys-48 is protonated, it can move out of the peroxide binding site, generating a peroxide-reactive open conformation. When Lys-48 is unprotonated, the open conformation is not accessible on the time scale of the peroxide binding experiments, and at these more alkaline pH values, His-181 deprotonates, generating the bis-imidazole form of CcP. Ionization of Lys-48 and His-181 are represented by pK_{E3} and pK_{E4}, respectively, in Figure 15. The apparent pK_A of Lys-48 is 6.8–6.9 in both buffer systems, and this is a reasonable value for deprotonation of the ϵ-amino group in the heme pocket. Normal pK_A values for the ϵ-amino group are about 9.5, but when the group moves toward the positively charged heme iron, as seen in the crystal structure (Figure 8), the protonated form is destabilized, decreasing the apparent pK_A.

In this mechanism, the actual value of the pH-independent rate constant for the hydrogen peroxide binding step cannot be determined; only the ratio k_a/k_{-i} can be determined (Table III). However, we know that k_{-i} must be at least 10 times larger than k_i, and we can establish lower limits for k_a of 19–28 μM^{-1} s^{-1} in the two buffer systems. These lower limits are about 50% the rate of reaction between CcP(YST) and hydrogen peroxide.

Nitrate Binding to CcP. The spectrum of CcP(YST) shows small differences at acidic pH, depending upon whether nitrate or phosphate is used to adjust the ionic strength (Conroy & Erman, 1978; Vitello *et al.*, 1990b). However, the kinetics of the hydrogen peroxide/CcP(YST) reaction are markedly different in nitrate-containing and phosphate buffers (Figure 6A; Loo & Erman, 1975; Balny *et al.*, 1987a). Our thesis is that nitrate binds in the heme pocket of CcP(YST), stabilizing the protonated form of His-52. His-52 promotes Compound I formation by acting as a general base, accepting a proton from hydrogen peroxide and allowing the peroxy anion to bind to the heme iron (Poulos & Kraut, 1980; Erman *et al.*, 1993). By stabilizing the protonated form of His-52, nitrate inhibits hydrogen peroxide binding at low pH, Figure 6A. The apparent pK_A of His-52 shifts from a value of about 4.0 in the absence of nitrate to 5.4 in the presence of 88 ± 8 mM nitrate.

Nitrate also inhibits the reaction between HRP and hydrogen peroxide in the same manner as it inhibits the CcP/hydrogen peroxide reaction (Araiso & Dunford, 1980), although the apparent pK_A for the group that effects the kinetics is shifted about 1.4 units to more acidic pH. The apparent pK_A for the catalytic group varies from about 2.5 in the absence of nitrate to 3.9 ± 0.1 in the presence of 100 mM nitrate. Araiso and Dunford observed a small spectral perturbation in the presence of nitrate which they used to

Table III: Kinetic Parameters for the Reaction between CcP(R48K) and Hydrogen Peroxide[a]

parameter	nitrate-containing buffer	0.1 M phosphate buffer
k_a/k_{-1} (M^{-1})	$(9.60 \pm 1.60) \times 10^4$	$(9.60 \pm 1.51) \times 10^4$
k_i (s^{-1})	204 ± 22	291 ± 34
pK_{E1}	3.66 ± 0.25	4.11 ± 0.12
pK_{E2}	5.36 ± 0.13	4.82 ± 0.15	
pK_{E3}	$6.90 \bullet 0.09$	6.76 ± 0.09
pK_{E4}	6.53 ± 0.14	6.89 ± 0.09

[a] Parameters defined in Figure 15 of text.

calculate an equilibrium dissociation constant for the HRP–nitrate complex of 200 mM at pH 4.45, about 10 times larger than that for the CcP–nitrate complex. They also showed that nitrate did not bind to the heme iron through competition experiments with cyanide.

Our present studies shed further light on the binding of nitrate to CcP and, perhaps, to peroxidases in general. The key observation is that nitrate does not perturb either the spectrum of CcP(R48L) or the hydrogen peroxide kinetics. This strongly suggests that CcP(R48L) has no detectable affinity for nitrate and that Arg-48 is required for nitrate binding in the heme pocket of CcP(YST). Nitrate does influence the spectrum of CcP(R48K) (Table I and Figure 6) and its kinetics with hydrogen peroxide (Table III and Figures 12 and 13), indicating that a positive charge at position 48 is the important determinant for nitrate binding.

CONCLUSIONS

The crystallographic structures of CcP(R48L) and CcP(R48K) have been determined and show only small changes from those of wild-type enzyme. The distal pocket of CcP(R48L) is open and consistent with exclusive pentacoordination of the heme iron. In CcP(R48K), Lys-48 moves toward the heme iron, displacing water-595, and occupies the putative peroxide binding site. It appears that the ϵ-amino group of Lys-48 does not bind to the heme iron in the crystal structure, but the electronic absorption spectrum suggests that CcP(R48K) has a small fraction of hexacoordinate component at neutral pH, consistent with previous resonance Raman studies (Smulevich *et al.*, 1989). The electronic absorption spectra of both CcP(R48L) and CcP(R48K) are dependent upon pH, and both form the typical alkaline bis-imidazole form of CcP, with His-52 coordinated to the heme iron. The apparent pK_A for formation of the bisimidazole form of CcP is 7.5 for CcP(R48L) and 6.9 for CcP(R48K).

Replacement of Arg-48 by Leu or Lys is consistent with the proposed role of Arg-48 in the mechanism of Compound I formation (Poulos & Kraut, 1980). Substitutions at position 48 should have little effect on the apparent bimolecular rate constant for the hydrogen peroxide/CcP reaction at low peroxide concentrations. This is observed, with the pH-independent bimolecular rate constant for the reaction with hydrogen peroxide being 0.82 μM^{-1} s^{-1} and greater than 28 μM^{-1} s^{-1} for the reaction with CcP(R48L) and CcP(R48K), respectively. These values are about 55- and 2-fold smaller than observed for CcP(YST) but still 3.5–5 orders of magnitude faster than the reaction of metmyoglobin with hydrogen peroxide (Yonetani & Schleyer, 1967).

The observed pseudo-first-order rate constant for the hydrogen peroxide reaction saturates at high hydrogen peroxide concentrations for both mutants. However, the cause of the saturation is quite distinct for the two mutants. In CcP(R48L), the rate of the hydrogen peroxide reaction appears to be limited by the oxygen–oxygen bond scission step, with a rate in the range of 1000–1950 s^{-1}, an estimated 2 orders of magnitude slower than for wild-type enzyme. In CcP(R48K), the peroxide reaction may be limited by a conformational-gating step, with a rate of 200 to 290 s^{-1} in nitrate-containing and phosphate buffers, respectively. The conformational gating may be associated with movement of Lys-48 out of the peroxide binding site or, possibly, rotation of His-52 to bring it into a position where it can interact with the incoming hydrogen peroxide.

Replacement of Arg-48 with either leucine or lysine residues reduces the stability of Compound I. Compounds I of both CcP(R48L) and CcP(R48K) decay 2–3 orders of magnitude more rapidly than CCP(YST) Compound I. The endogenous decay of CcP(YST) Compound I is quite complex (Erman & Yonetani, 1975a,b), and the mechanism for reduction of the Trp-191 radical and the Fe(IV) site is unknown. Alterations in the distal pocket, especially the hydrogen-bonding pattern of Arg-48, could be important factors is stabilizing Compound I.

ACKNOWLEDGMENT

The authors to thank Drs. Herbert Axelrod and Noam Adir for recording the absorption spectrum of crystalline CcP(R48K).

REFERENCES

Araiso, T., & Dunford, H. B. (1980) *Biochem. Biophys. Res. Commun. 94*, 1177–1182.

Balny, C., Anni, H. S., & Yonetani, T. (1987a) *FEBS Lett. 221*, 349–354.

Balny, C., Travers, F., Barman, T., & Douzou, P. (1987b) *Eur. Biophys. J. 14*, 375–383.

Chance, B., DeVault, D., Legallais, V., Mela, L., & Yonetani, T. (1967) in *Fast Reactions and Primary Processes in Chemical Kinetics* (Claesson, S., Ed.), pp 437–468, Interscience Publishers, New York.

Conroy, C. W., & Erman, J. E. (1978) *Biochim. Biophys. Acta 527*, 370–378.

Dhaliwal, B. K., & Erman, J. E. (1985) *Biochim. Biophys. Acta 827*, 174–182.

Edwards, S. L., & Poulos, T. L. (1990) *J. Biol. Chem. 265*, 2588–2595.

Erman, J. E. (1974a) *Biochemistry 13*, 34–39.

Erman, J. E. (1974b) *Biochemistry 13*, 39–44.

Erman, J. E., & Yonetani, T. (1975a) *Biochim. Biophys. Acta 393*, 343–349.

Erman, J. E., & Yonetani, T. (1975b) *Biochim. Biophys. Acta 393*, 350–357.

Erman, J. E., Vitello, L. B., Miller, M. A., & Kraut, J. (1992) *J. Am. Chem. Soc. 114*, 6592–6593.

Erman J. E., Vitello, L. B., Miller, M. A., Shaw, A., Brown, K. A. & Kraut, J. (1993) *Biochemistry* (preceding paper in this issue).

Fishel, L. A., Villafranca, J. E., Mauro, J. M., & Kraut, J. (1987) *Biochemistry 26*, 351–360.

Iizuka, T., & Yonetani, T. (1970) *Adv. Biophys. J. 1*, 157–182.

Kolthoff, I. M., & Belcher, R. (1957) in *Volumetric Analysis*, Vol. III, pp 75–76, Interscience, New York.

Kresheck, G. C., & Erman, J. E. (1988) *Biochemistry 27*, 2490–2496.

Lent, B., Conroy, C. W., & Erman, J. E. (1976) *Arch. Biochem. Biophys. 177*, 56–61.

Loo, S., & Erman J. E. (1975) *Biochemistry 14*, 3467–3470.

Miller, M. A., Coletta, M., Mauro, J. M., Putnam, L. D., Farnum, M. F., Kraut, J., & Traylor, T. G. (1990) *Biochemistry 29*, 1772–1791.

Poulos, T. L., & Kraut, J. (1980) *J. Biol. Chem. 255*, 8199–8205.

Satterlee, J. D. & Erman J. E. (1980) *Arch. Biochem. Biophys. 202*, 608–616.

Smith, D. W., & Williams, R. J. P. (1968) *Biochem. J. 110*, 297–301.
Smulevich, G. Mauro, J. M., Fishel, L. A., English, A. M., Kraut, J., and Spiro, T. G. (1988) *Biochemistry 27*, 5477–5485.
Smulevich, G., Mantini, A. R., English, A. M., & Mauro, J. M. (1989) *Biochemistry 28*, 5058–5064.
Smulevich, G., Miller, M. A., Kraut, J., & Spiro, T. (1991) *Biochemistry 30*, 9546–9558.
Vitello, L. B., Erman, J. E., Mauro, J. M., & Kraut, J. (1990a) *Biochim. Biophys. Acta 1038*, 90–97.
Vitello, L. B., Huang, M., & Erman, J. E. (1990b) *Biochemistry 29*, 4283–4288.
Vitello, L. B., Erman, J. E. Miller, M. A., Mauro, J. M., & Kraut, J. (1992) *Biochemistry 31*, 11524–11535.
Wang, J. (1988) Ph.D. Dissertation, University of California, San Diego.
Wang, J., Mauro, J. M., Edwards, S. L., Oatley, S. J., Fishel, L. A., Ashford, V. A., Xuong, N.-H., & Kraut, J. (1990) *Biochemistry 29*, 7160–7173.
Xuong, N.-H., Nielsen, C. P., Hamlin, R., & Anderson, D. H. (1985) *J. Appl. Crystallogr. 18*, 342–350.
Yonetani, T., & Schleyer, H. (1967) *J. Biol. Chem. 242*, 1974–1979.
Yonetani, T., & Anni, H. (1987) *J. Biol. Chem. 262*, 9547–9554.